Ab initio study of the HO 2 + NO reaction: Prediction of the total rate constant and product branching ratios for the forward and reverse processes

R. S. Zhu and M. C. Lin

Citation: The Journal of Chemical Physics **119**, 10667 (2003); doi: 10.1063/1.1619373
View online: http://dx.doi.org/10.1063/1.1619373
View Table of Contents: http://scitation.aip.org/content/aip/journal/jcp/119/20?ver=pdfcov
Published by the AIP Publishing

Ab initio study of the HO_2+NO reaction: Prediction of the total rate constant and product branching ratios for the forward and reverse processes

R. S. Zhu and M. C. Lin[a)]
Department of Chemistry, Emory University, Atlanta, Georgia 30322

(Received 13 June 2003; accepted 26 August 2003)

The mechanisms for HO_2+NO and its reverse reactions have been investigated by *ab initio* molecular orbital and transition-state theory calculations. The species involved have been optimized at the B3LYP/6-311+G($3df$,$2p$) level and their energies refined by single-point calculations with the highest scheme of the modified Gaussian-2 method. *Ab initio* results show that formation of $HO+NO_2$ from HO_2+NO by the direct fragmentation of the peroxynitrous acid, HOONO intermediate, is predominant; the alternative path occurring by the isomerization of HOONO to $HONO_2$ is 5.2 kcal/mol less favorable. The stepwise formation of $HNO+O_2$ from HOONO is energetically unfavorable; the barriers for the direct H abstract reactions via singlet and triplet paths are found to be rather high also. Rate constant calculations show that the forward reaction is pressure independent below 10 atm; the reverse $OH+NO_2$ reactions producing $HONO_2$ and HOONO appear to be strongly pressure dependent; below 1 atm, the yield of HOONO from $HO+NO_2$ is $<2.5\%$ at 300–400 K, it reaches 12.2% and 9.1%, respectively, at 300 and 400 K at 3.8×10^4 Torr pressure. The low- and high-pressure rate constants with He as a third-body for the formation of HOONO and $HONO_2$ from the $HO+NO_2$ reaction can be expressed by k^0 (HOONO)$=3.15\times10^2\ T^{-12.3}\exp(-585/T)$, k^0 ($HONO_2$)$=3.32\times10^{-6}\ T^{-8.8}\exp(-1569/T)$ $cm^6\,molecule^{-2}\,s^{-1}$ and k^∞ (HOONO)$=1.71\times10^{-10}\ T^{-0.24}\exp(100/T)$ and k^∞ ($HONO_2$)$=4.74\times10^{-9}\ T^{-0.82}\exp(21/T)$ $cm^3\,molecule^{-1}\,s^{-1}$, respectively, in the temperature range of 200–2000 K. The unimolecular decomposition rate constant (in Ar) of HNO_3 can be expressed as k_d^∞ (HNO_3)$=2.30\times10^{23}\ T^{-2.27}\exp(-26317/T)\ s^{-1}$ and k_d^0 (HNO_3)$=1.27\times10^{15}\ T^{-6.55}\exp(-26038/T)$ $cm^3\,molecule^{-1}\,s^{-1}$, respectively. The predicted values are all in close agreement with experimental data for both forward and reverse processes. © *2003 American Institute of Physics.* [DOI: 10.1063/1.1619373]

I. INTRODUCTION

The reaction of HO_2 and NO plays a very important role in the chemistry of Earth's atmosphere. Experimentally, there have been numerous studies on its forward[1–19] and reverse[20–50] processes, whose key references will be cited and compared with our theoretically predicted values later. Theoretically, there are several calculations[51–59] related to this reaction system; most of the investigators[51–55] focus mainly on the structures and vibrational frequencies of various conformers of HOONO (peroxynitrous acid) or HNO_3 using different methods. For the potential energy surface (PES), Sumathi and Peyerimhoff[57] have investigated it at the B3LYP/6-311++G(d,p) level with part of the points calculated at the MP2/6-311++G(d,p) or the CAS(8,8)/6-31G(d) or G2 level; Chakraborty and Lin[58] reported part of the PES which was relevant to the $OH+NO_2$ recombination and the HNO_3 decomposition processes at the G2M(CC5) level; and Dixon *et al.*[55] investigated the decomposition of HOONO at the CCSD(T)/CBS level. In addition, McGrath and Rowland,[56] Dransfield *et al.*,[26] Donahue *et al.*,[25] and Jin *et al.*[59] have studied the isomerization processes among the HOONO isomers at the MP2/6-31G(d), B3LYP/6-31G(d,p), B3LYP/6-31G(d,p), and B3LYP/6-311+G(d,p) levels, respectively. To our knowledge, a complete PES of the system has not yet been evaluated at a high level, neither a full calculation of rate constants for the forward and reverse processes based on the complete PES.

The major goal of this work lies in the characterization of the PES using the highest scheme of the G2M method[60] and in the quantitative prediction of the effects of P and T on the total and product branching rate constants for the forward and reverse reactions. The predicted values over a wide range of conditions will be fully compared with existing experimental data.

II. COMPUTATIONAL DETAILS

The geometries of the reactants, products, intermediates and transition states of the title reactions were fully optimized by using the hybrid density functional B3LYP method (Becke's three-parameter nonlocal exchange functional[61–63] with the correlation functional of Lee, Yang, and Parr[64]) with

a)Author to whom correspondence should be addressed. Electronic mail: chemmcl@emory.edu

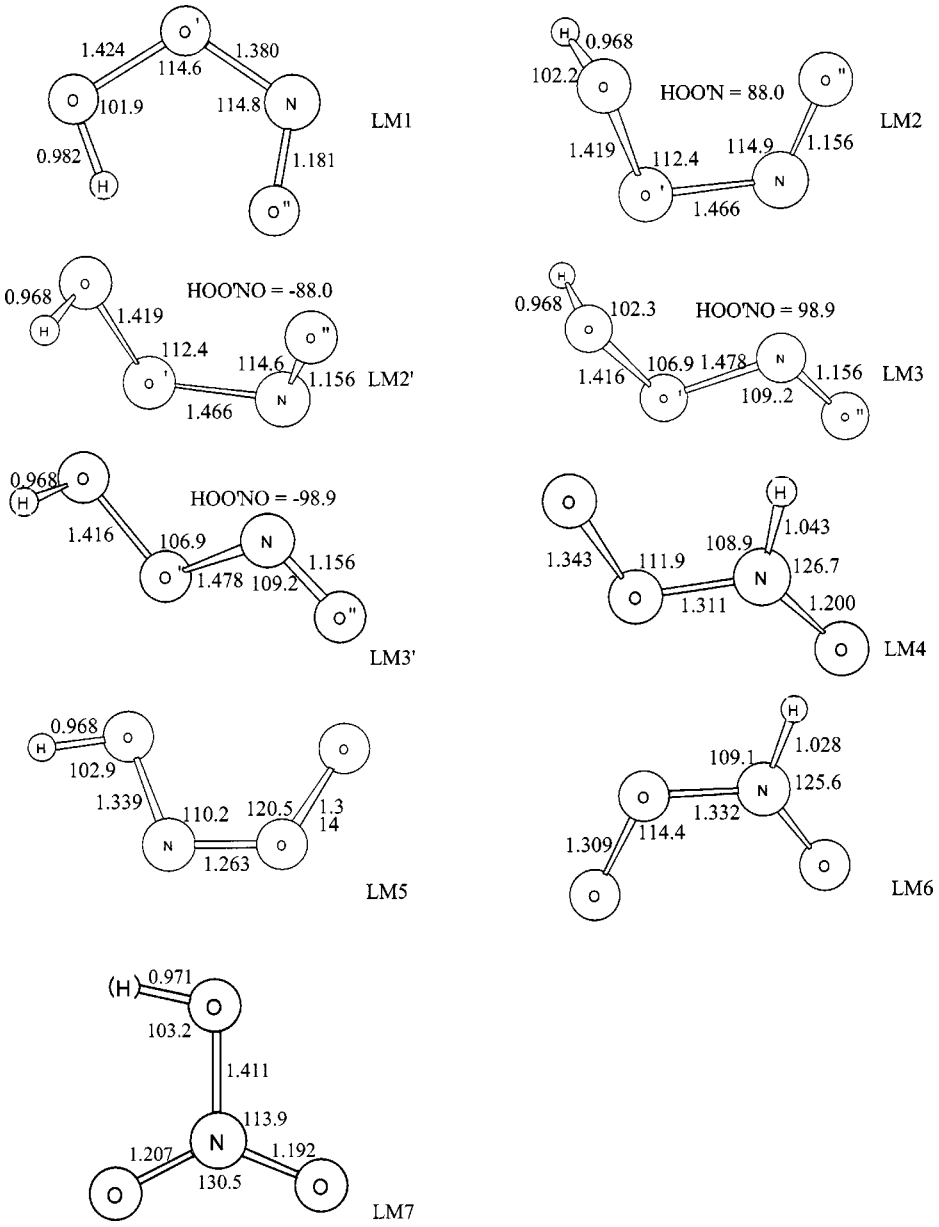

FIG. 1. The optimized geometry of intermediates computed at the B3LYP/6-311+G(3df,2p) level for the HO_2+NO system.

the 6-311+G(3df,2p) basis set. Vibrational frequencies employed to characterize stationary points, zero-point energy (ZPE) corrections have also been calculated at this level of theory, and have been used for the rate constant calculations. Intrinsic reaction coordinate (IRC) calculations[65] have been performed to confirm the connection of each transition state with designated intermediates. The single point energies are refined by using the highest scheme of the G2M method, G2M (CC1).[60] All calculations were carried out with GAUSSIAN 98.[66]

The rate constants were computed with a variational RRKM [Variflex (Ref. 67)] code which solves the master equation,[68,69] involving multistep vibrational energy transfers for the excited intermediate $HONO_2^*$ or HOONO*. For the coupling of multiwells, the ChemRate code of Mokrushin *et al.*[70] was employed.

III. RESULTS AND DISCUSSION

A. Potential energy surface and reaction mechanism

The optimized geometries of the intermediates and transition states are shown in Figs. 1 and 2, respectively. The potential energy diagram obtained at the G2M(CC1)//B3LYP/6-311+G(3df) level[60] is presented in Fig. 3. The predicted vibrational frequencies and rotational constants are summarized in Table I to compare with the available experimental vibrational frequencies of HOONO isomers.

1. Isomers of HOONO

a. Equilibrium geometries and frequencies: As mentioned above, the structural parameters and vibrational frequencies of HOONO isomers have been investigated and compared with those predicted by several groups.[51–55] There are three stable peroxynitrous acid isomers, LM1–LM3;

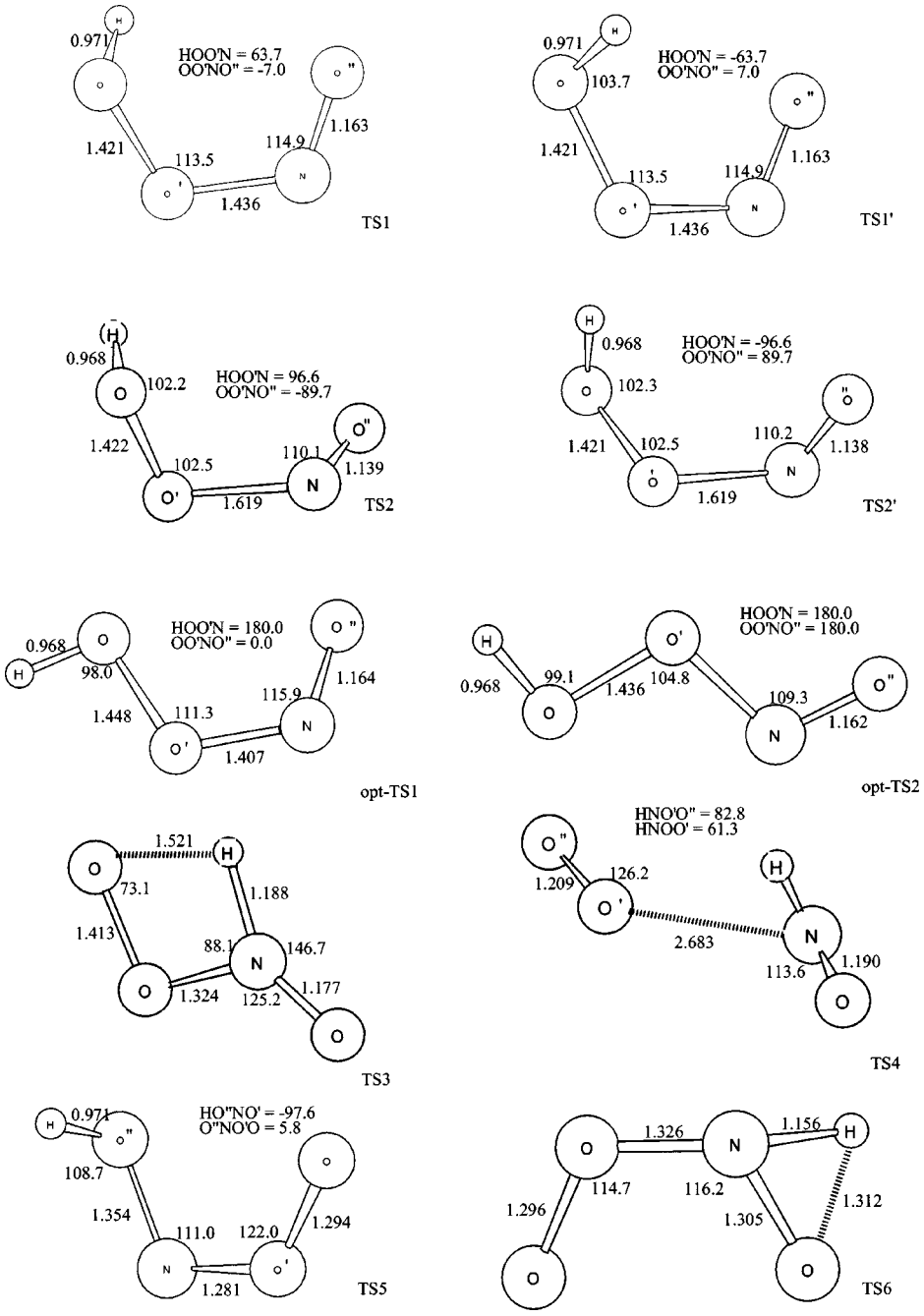

FIG. 2. The geometry of the transition states involved in the HO_2+NO reaction computed at the B3LYP/6-311+G($3df,2p$) level.

among them, *cis,cis*-HOONO (LM1) was predicted to be the most stable one by all of the authors. For the three isomers, the predicted structural parameters at the B3LYP/6-311 +G($3df,2p$) level in this work are in reasonable agreement with the results obtained by other authors.[51–55] Taking LM1 as an example, our predicted bond lengths of HO, OO′, O′N, and NO″ (see LM1 in Fig. 1), 0.982, 1.426, 1.380, and 1.181 Å, are close to the values of 0.982, 1.426, 1.391, and 1.188 Å obtained at the highest level, QCISD(T)/cc-pVQZ used by Li and Francisco.[52] There are slight deviations by comparing the values of 0.955, 1.428, 1.379, and 1.178 Å predicted by Sumathi and Peyerimhoff[57] at the CAS (8,8)/6-31(d,p) level. The calculated frequencies are also close to the experimental values[71] (see Table I); the maximum deviation between our calculated and the experimental values is only around 7%. The comparison of the calculated molecular parameters by different methods with several basis sets can be found in Refs. 51, 52, and 59. From previous calculations,[72–77] we learn that the molecular parameters predicted by density function theory (DFT) with large basis sets are fairly reliable. In the later rate constant calculations, those structural parameters obtained at the B3LYP/6-311 +G($3df,2p$) level and the energies at the G2M(CC1) will be used. In addition, the optical isomers LM2′ and LM3′ corresponding to LM2 and LM3, and some other unrelated isomers (LM4–LM7) were located; their structures are also shown in Fig. 1.

b. Relative energies: The energies cited in the following text are the G2M values. For the isomers and related isomerization transition states, the higher level correction (HLC) is

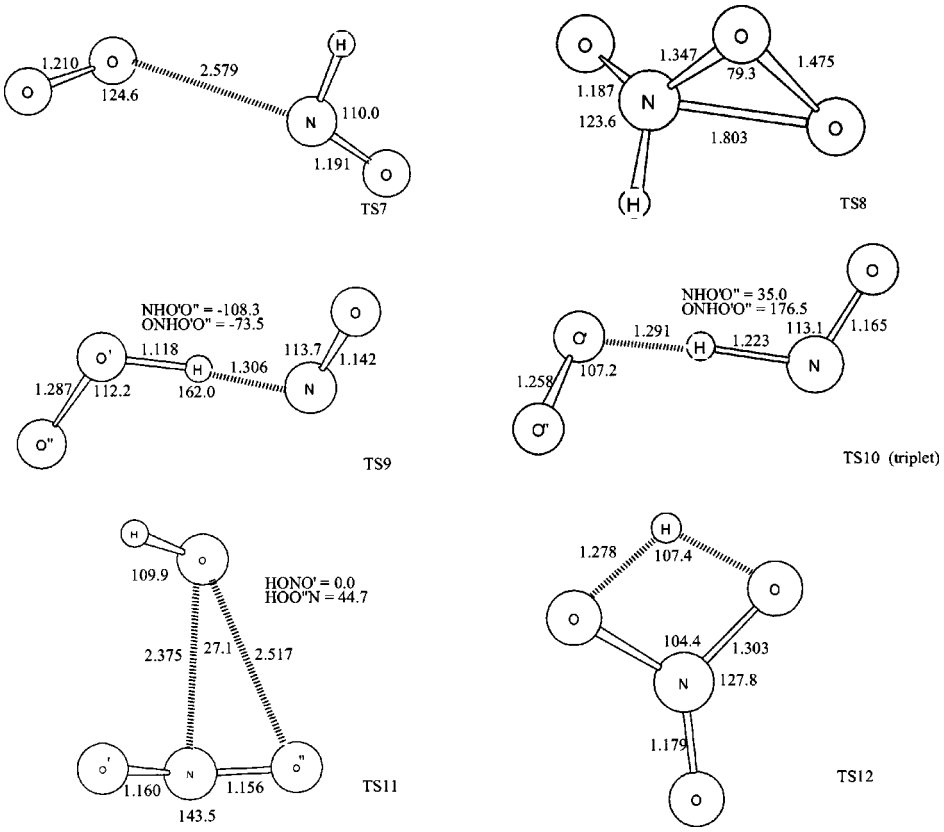

FIG. 2. (*Continued.*)

identical in the G2M scheme because they have equal α and β valence electrons. The main corrections are those for diffuse functions, higher polarizations on nonhydrogen atoms and the electron correlation by the coupled cluster method. The total corrections for the isomers or related transition states are different because of their different configurations. The relative energies of the three conformers, *cis*,*cis*-HOONO (LM1), *cis*,perp-HOONO (LM2) and *trans*, perp-HOONO (LM3) are 0.0, 0.6, and 2.5 kcal/mol at the G2M (CC1) level, which agree well with the values, 0.0, 0.7, 2.8 kcal/mol,[56] 0.0, 0.66, 2.71 kcal/mol,[59] and 0.0, 1.2, 3.1 kcal/mol (without zero point correction)[56] obtained at the QCISD(T)/6-311G(d,p), MP2/6-311++G($3df,2p$) and G2 levels, respectively. The dissociation energies predicted at 0 K, D_0 (HO-ONO), for LM1–LM3 are 20.5, 19.9, and 18.0 kcal/mol at the G2M (CC1) level. The calculated bond energies D_0 (HO–ONO) for the three isomers are close to the most recent experimentally determined value, $D_0 = 19.8 \pm 0.23$ kcal/mol (Ref. 23) and the values $D_0 = 20.3$ (Ref. 57) and 18.8 kcal/mol (Ref. 52) predicted at the G2 and CBS-

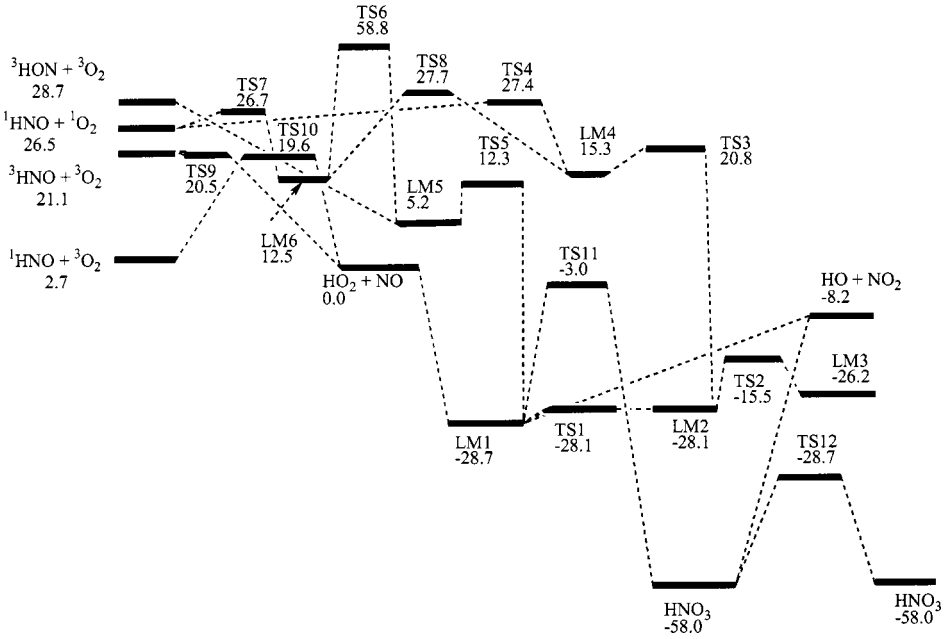

FIG. 3. The schematic diagram of the potential energy surface for the HO_2–NO system computed at the G2M (CC1) level.

TABLE I. Rotational constants and vibrational frequencies of the intermediates and transition states predicted at the B3LYP6-311+G(3*df*,2*p*) level.

	B3LYP/6-311+G(3*df*,2*p*)	
Species	I_a, I_b, I_c (GHz)	Frequencies (cm^{-1})
LM1[a]	21.9, 7.9, 5.8	355.3, 373.3, 512.5, 664.6 (629.1), 845.5 (794.3), 966.8 (927.1), 1452.6 (1395.0), 1667.0 (1600.3), 3532.4 (3285.4)
LM2	21.9, 7.3, 5.6	166.6, 323.7, 392.1, 474.6, 831.0, 965.9, 1392.3, 1790.3, 3739.6
LM3	55.5, 4.9, 4.6	213.9, 302.8, 363.7, 470.0, 810.0, 1019.9, 1418.0, 1805.5, 3752.8
LM4	67.1, 5.2, 4.8	242.9, 401.5, 655.0, 870.9, 920.4, 1154.6, 1382.8, 1623.5, 3187.9
LM5	22.6, 8.1, 5.9	381.3, 525.3, 594.7, 827.9, 1062.3, 1082.9, 1191.2, 1448.3, 3765.2
LM6	24.5, 7.5, 5.7	326.1, 511.4, 611.9, 854.9, 945.9, 1062.0, 1448.4, 1607.8, 3367.2
LM7	13.1, 12.1, 6.3	493.2, 588.7, 654.6, 787.8, 903.3, 1325.1, 1350.6, 1755.8, 3735.1
TS1	21.9, 7.5, 5.7	199.2 *i*, 330.4, 407.6, 533.7, 837.1, 957.9, 1411.9, 1753.9, 3714.9
TS2	25.9, 5.7, 5.2	255.2 *i*, 269.4, 414.9, 465.2, 716.1, 940.5, 1385.8, 1877.9, 3740.7
TS3	52.9, 5.6, 5.0	1396.8 *i*, 210.2, 525.6, 721.4, 838.4, 1130.7, 1205.5, 1724.6, 2236.9
TS4	49.2, 2.5, 2.4	332.8 *i*, 47.9, 59.2, 83.6, 158.0, 1494.3, 1568.7, 1674.2, 2819.6
TS5	21.9, 7.9, 5.9	626.2 *i*, 384.4, 530.4, 849.7, 1038.9, 1073.2, 1130.9, 1258.4, 3710.1
TS6	23.0, 7.9, 5.9	1932.3 *i*, 283.8, 325.1, 534.8, 803.2, 875.4, 1121.9, 1307.6, 2632.0
TS7	49.0, 2.4, 2.4	68.1 *i*, 51.4, 72.6, 103.5, 240.4, 1523.2, 1573.9, 1690.9, 2897.9
TS8	25.4, 7.2, 6.3	116.3 *i*, 524.2, 662.3, 778.1, 849.8, 1110.9, 1455.2, 1645.6, 3351.6
TS9	47.4, 3.1, 2.9	565.2 *i*, 81.1, 112.2, 282.1, 577.5, 940.0, 1383.9, 1555.3, 1930.3
TS10	39.7, 3.1, 2.9	1679.4 *i*, 29.6, 110.8, 260.1, 574.3, 888.8, 1411.4, 1554.9, 1817.9
TS11	12.4, 7.4, 4.8	700.9 *i*, 141.0, 227.0, 285.4, 518.8, 653.7, 1344.2, 1997.6, 3796.9
TS12	14.9, 11.5, 6.5	1946.2 *i*, 628.5, 748.2, 847.7, 1061.5, 1117.5, 1335.6, 1671.5, 2319.6

[a]Frequencies in the parentheses are taken from Ref. 71.

limit levels, respectively. However, at the MP2/6-311++G(*d*,*p*), B3LYP/6-311++G(*d*,*p*), and QCISD/6-311++G(2*df*,2*pd*)//MP2/6-311++G(*d*,*p*) levels, the predicted values are 8.1, 14.6, and 17.6 kcal/mol (without ZPE correction),[57] and the underestimated dissociation energies may be ascribed to the insufficient electron correlation and the basis set truncation effects in the calculations.[52] For the D_0 (HOO–NO), our calculated values are 28.7, 28.1, and 26.2 kcal/mol for LM1, LM2, and LM3, respectively. These data are also close to the corresponding values of 28.8 and 28.4 kcal/mol (Ref. 57) obtained at the G1 and G2 levels. Again, the MP2/6-311++G(*d*,*p*), B3LYP/6-311++G(*d*,*p*), and QCISD/6-311++G(2*df*,2*pd*)//MP2/6-311++G(*d*,*p*) methods give significantly lower values: 25.4, 23.0, and 21.3 kcal/mol,[57] respectively. The optical isomers LM2 and LM2′, and LM3 and LM3′ have equal energies as predicted. Other unrelated isomers, LM4–LM6 lie above the reactants by 5.2, 15.3, and 12.5 kcal/mol. LM7 ($HONO_2$) related to the reverse reaction lies below the reactants by 58.0 kcal/mol; it is the most stable isomer in the global $H_1N_1O_3$ system.

c. Isomerization: At the G2M (CC1) level, the isomerization barrier height from LM1 to LM2 via TS1 is only 0.6 kcal/mol corresponding to the rotation around the OO′ bond; from LM2 to LM3, it has to overcome 12.6 kcal/mol barrier via TS2. These values are consistent with the data of 0.8 and 12.8 kcal/mol,[56] 0.90 and 13.4 kcal/mol,[59] and 1.6 and 12.5 kcal/mol (Ref. 57) obtained at the MP2/6-31G(*d*), B3LYP/6-311+G(*d*,*p*), and B3LYP/6-311++G(*d*,*p*) levels, respectively. The barriers for LM1 to LM2′ and LM2′ to LM3′ are also 0.6 and 12.6 kcal/mol, respectively, via TS1′ and TS2′ as shown in Fig. 2. The opt-TS1 and opt-TS2 correspond to the transition states between optical isomers LM2↔LM2′ and LM3↔LM3′ with the barrier

heights of 1.6 and 2.0 kcal/mol, respectively; their energies are not plotted in Fig. 3. Another critical isomerization from HOONO to $HONO_2$ will be addressed later.

2. $^{1,3}HNO+^{1,3}O_2$ and $^{3}HON+^{3}O_2$ formation

The results obtained at the B3LYP/6-311++G(d,p) level by Sumathi and Peyerimhoff[57] indicated that the HNO formation cannot occur via the association-elimination process. Recently, Dixon *et al.*[55] reported that HOONO can decompose to $HNO+O_2$ ($^1\Delta_g$) via a four-center transition state at the CCSD(T)/CBS//MP2/cc-pVTZ level. In our calculation at the B3LYP/6-311+G($3df,2p$) level, a similar four-center transition state (TS3) was located, but our IRC (Ref. 65) analysis shows that TS3 actually connects LM2 with another stable intermediate LM4, whose decomposition via TS4 produces $^1HNO+^1O_2$ with a 12.1 kcal/mol barrier. Our result is consistent with that of Sumathi and Peyerimhoff.[57] To clarify the possible effect of MP2 and DFT methods on the TS3 structure, we calculate the same TS at the MP2/6-311(d,p) level, the IRC result confirms the above conclusion.

From Fig. 3 we see that LM1 can isomerize to LM5 via TS5. TS5 and LM5 lie above the reactants by 12.3 and 5.2 kcal/mol, respectively. The latter can directly dissociate to $HON+O_2$ or isomerize to LM6 with a very high barrier height, 53.6 kcal/mol (TS6); this intermediate (LM6) can further dissociate to the $^1HNO+^1O_2$ via TS7 with 14.2 kcal/mol barrier. LM4 and LM6 are connected by TS8, which corresponds to the rotation of the O–O group around the N–O bond with 12.4 kcal/mol barrier above LM4; this barrier is close to the value, 12.6 kcal/mol, for the rotation of the NO″ group in LM2 around the N–O′ bond to form LM3 via TS2 (see Fig. 2). Apparently, $^1HNO+^1O_2$ formation cannot occur by the direct decomposition of HOONO; the indirect process as described is unfavorable because of the high isomerization barriers. Figure 3 also shows the direct abstraction channels, $HOO+NO\rightarrow{}^{1,3}HNO+{}^3O_2$, via singlet (TS9) and triplet (TS10) states. At the G2M (CC1) level, their barriers are predicted to be 20.5 and 19.6 kcal/mol, respectively; the former is slightly lower than the energy of the products (21.1 kcal/mol) suggesting that the reverse barrier should be negligible. Kinetically, these channels are not expected to be important even at high temperatures because of their large barriers.

3. $HO+NO_2$ formation

There are two possible pathways for the formation of $HO+NO_2$ from HO_2+NO; one is the direct dissociation of the HOONO intermediate and the other is the isomerization of HOONO first to $HONO_2$, followed by O–N fission to produce $HO+NO_2$. The isomerization barrier for HOONO to $HONO_2$ has been controversial: Sumathi and Peyerimhoff[57] reported a barrier of 39.0 kcal/mol at the B3LYP/6-311++G(d,p) level, which may be compared with the value of Dixon *et al.*,[55] 21.4 kcal/mol above HOONO at the CBS//MP2/ccpVTZ level. Our result obtained at the G2M (CC1)//B3LYP/6-311+G($3df,2p$) level shows that the transition state (TS11) lies 25.7 kcal/mol above HOONO, or 5.2 kcal/mol higher than that of the dissociation products, $HO+NO_2$. Most recently, a very detailed calculation carried out by Nguyen *et al.*[78] shows that for a similar isomerization reaction from H_3C-ONO to H_3C-NO_2 its transition state lies 6 kcal/mol above the CH_3+NO_2 asymptote, which is very close to our value of 5.2 kcal/mol for the isoelectronic HO–ONO system. To complete the PES, the transition state (TS12) for H migration within HNO_3 is also located as shown in Figs. 2 and 3.

B. Rate constant calculations

Variational TST and RRKM calculations have been carried out for the reactions of HO_2+NO and its reverse process, $HO+NO_2$. The L-J parameters required for the RRKM calculations for the quenching of HOONO or $HONO_2$ were approximated by $\varepsilon/k=390$ K and $\sigma=4.24$ Å (Ref. 79) and those for He, N_2, and Ar: $\varepsilon/k=10$, 82.0, and 114 K and $\sigma=2.55$, 3.74, and 3.47 Å, respectively, were taken from the literature.[80]

1. Rate constants for the reaction of $HO_2+NO\leftrightarrow HO+NO_2$

Experimentally, Howard[10,15] extensively measured the rate constants for both directions by means of the laser magnetic resonance technique; Molina and co-workers[4] reported the rate constants for the forward reaction $HO_2+NO\rightarrow HO+NO_2$ and indicated that the reaction was pressure-independent. From the PES (Fig. 3), we see that the formation and decomposition of the HOONO (LM1) intermediate do not have well-defined transition states.

The forward reaction was first computed at 300 and 1000 K with the CHEMRATE code[70] coupling the intermediates involved in the reaction as follows:

$$
\begin{aligned}
HO_2+NO &\overset{k-1}{\leftrightarrow} LM1^* \overset{k1}{\rightarrow} LM1(+M)\\
&\overset{k2}{\rightarrow} HO+NO_2\\
&\overset{k3}{\leftrightarrow} HNO_3^* \overset{k5}{\rightarrow} HNO_3(+M)\\
&\qquad\overset{k6}{\rightarrow} HO+NO_2\\
&\overset{k4}{\leftrightarrow} LM3^* \overset{k7}{\rightarrow} LM3(+M)\\
&\qquad\overset{k8}{\rightarrow} HO+NO_2.
\end{aligned}
$$

In the above scheme, "$*$" represents internal excitation. In the CHEMRATE calculation, the transition state parameters for the barrierless association and decomposition processes were evaluated canonically for each temperature and critical separation, $r^{\#}(T)$, based on the maximum Gibbs free energy criterion as described previously for radical–radical reactions.[81,82]

The results show that under the conditions of 300 and 1000 K at 1 atm pressure, the formation of $HO+NO_2$ is dominant, the total deactivation rate for the intermediates is $<1\%$. At 10 000 atm, k_1 is about 98% of the total rate.

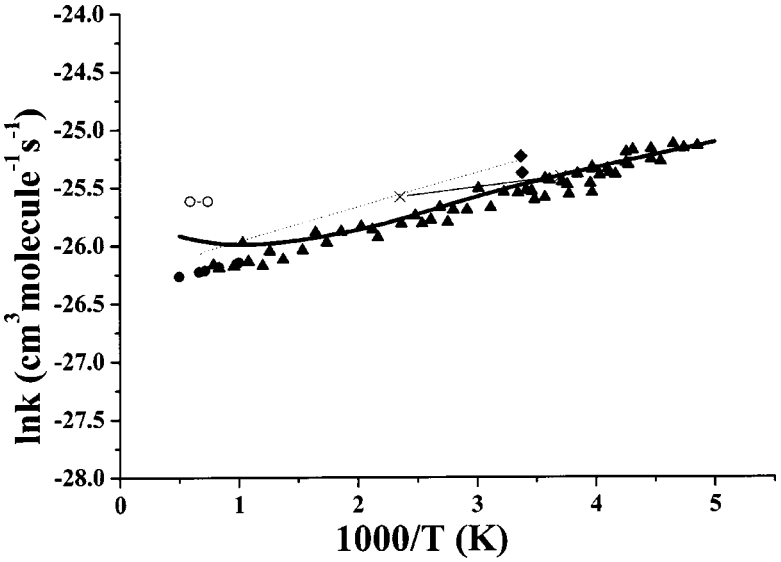

FIG. 4. Comparison of the predicted second-order temperature dependent rate constants for $HO_2+NO\rightarrow HO+NO_2$ with experimental values. Solid line is the predicted value in this work, dotted line is the results obtained by canonical variational approach in Ref. 58. ▲, Ref. 4; △, Refs. 10, 15; ○, Ref. 46; ●, Ref. 20, ◆, Ref. 12; ×, Ref. 14.

Based on this information, the rate constants for the rest of temperatures were calculated only based on the following scheme:

$$HO_2+NO \overset{k-1}{\leftrightarrow} LM1^* \overset{k1}{\rightarrow} LM1(+M)$$

$$\overset{k2}{\rightarrow} HO+NO_2.$$

Figure 4 shows the comparison of our predicted and experimental results for the forward reaction of $HO_2+NO\rightarrow HO+NO_2$ at 1 atm. The agreement between theory and experiment is excellent. It should be mentioned that below 10 atm, the formation of $HO+NO_2$ is pressure-independent. At temperatures above 1000 K, where experimental data are scattered, theory predicts a slight upturn of the rate constant due to the rapid increase in the values of partition functions associated with product formation.

For the reverse reaction $HO+NO_2\rightarrow HOONO\rightarrow HO_2+NO$, the rate constant for product formation was calculated with the VARIFLEX code by treating the process as a single well, $HO+NO_2\rightarrow LM1^*\rightarrow HO_2+NO$, because the isomerization barrier height from HNO_3 to HOONO (LM1) is much higher (see Fig. 3). For the barrierless transition states, the Morse potential, $E(R)=D_e[1-e^{-\beta(R-Re)}]^2$ was used to represent the stretching potential energy along the minimum energy path of each individual reaction coordinate. The β value of 3.13 $Å^{-1}$ for the entrance channel was obtained at the B3LYP/6-311++G(d,p) level. For the exit channel, however, the DFT method gave rise to scattered energies along the reaction minimum energy path, the CASSCF/(4,4)/6-31+G(d) method was employed to calculate the energies (De) which led to a reasonably smooth potential curve with $\beta=2.62$ $Å^{-1}$. As both B3LYP and CASSCF dissociation energies are not reliable, they were approximately scaled with the G2M values. In addition, the Lennard-Jones pairwise potential and the angularly anisotropic potential are also included in the final potential for rate constant calculation by the VARIFLEX code.

The predicted and experimental results are compared in

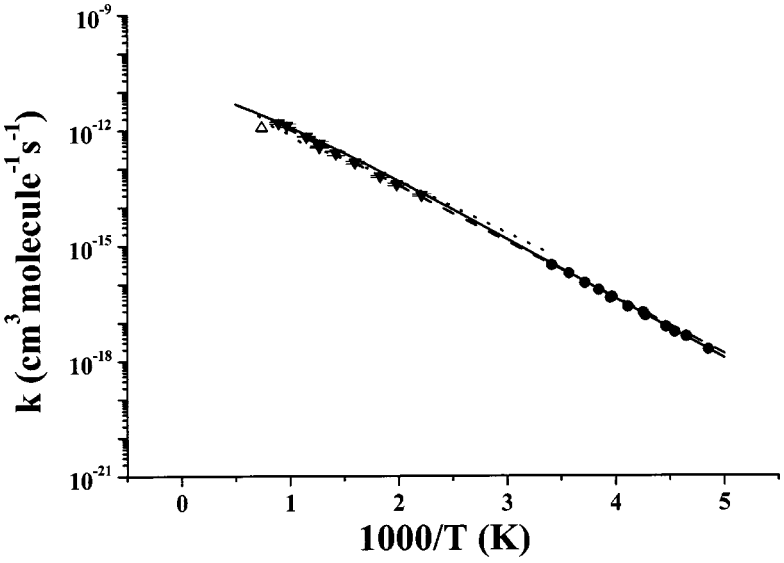

FIG. 5. Comparison of the predicted second-order temperature dependent rate constants for $HO+NO_2\rightarrow HO_2+NO$ with experimental values. Solid line is predicted value in this work, dotted line is the result obtained by canonical variational approach in Ref. 58, dashed line is taken from the equation in Ref. 31. ▼, Ref. 10; △, Ref. 46; ●, Ref. 4.

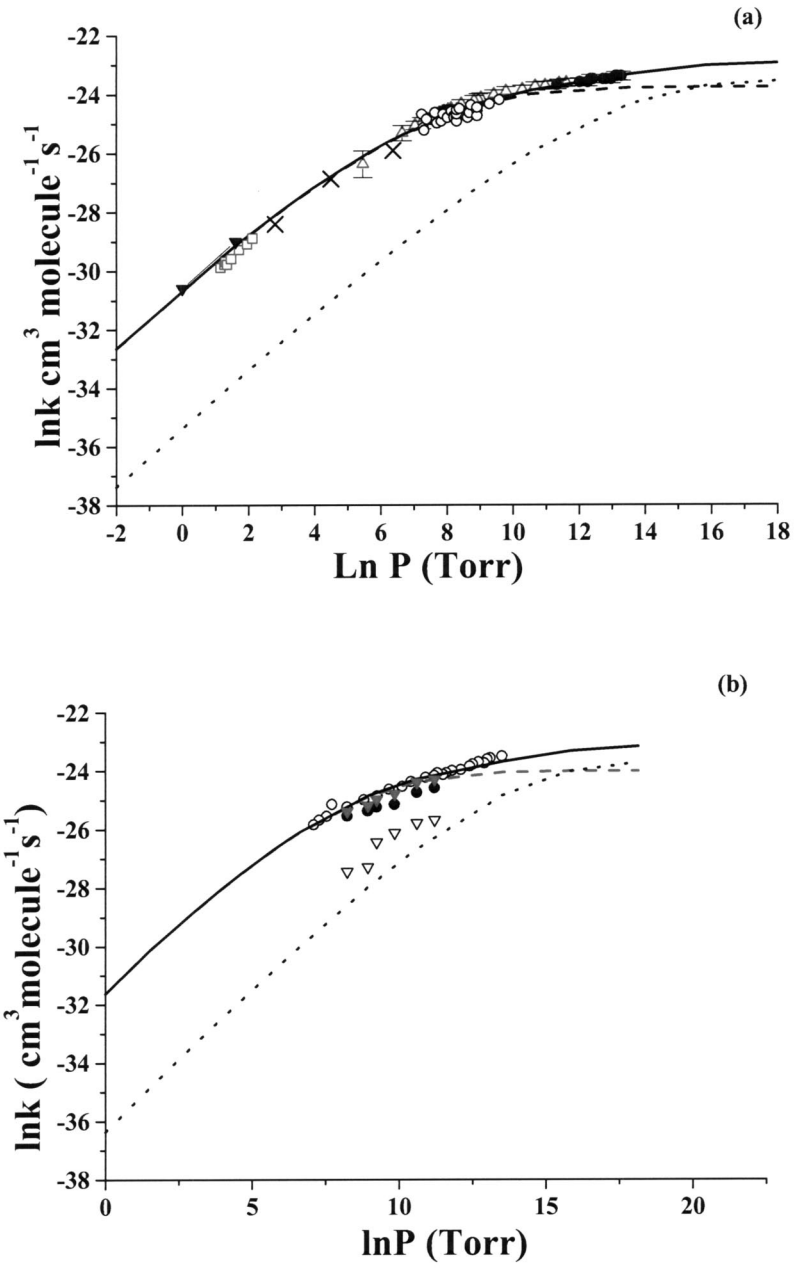

FIG. 6. Comparison of the predicted second-order pressure dependent rate constants for $HO+NO_2$ (in He) with experimental values. (a) 300 K, dashed, dotted, and solid curves are the predicted values in this work for the formation of $HONO_2$, HOONO, and the total rate, respectively. Symbols are the total experimental association rates: △, Ref. 30; ×, Ref. 35; ●, Ref. 27; ○, Ref. 40; ▼, Ref. 33. (b) 400 K, the meanings of dashed, dotted, and solid curves are the same as those in (a), symbols are experimental data, ○, Ref. 27; ▽, Ref. 23 for formation of HOONO at 430 K; ●, Ref. 23 for formation of $HONO_2$ at 430 K; ▼, Ref. 23, total association rate at 430 K.

Fig. 5. For comparison, the experimental values in Fig. 5 at low temperatures are obtained by converting the forward reaction rates[4] using the calculated equilibrium constants based on the molecular parameters calculated in our work with the heat of reaction, −7.5 kcal/mol. The results presented in Fig. 5 show an excellent agreement between theory and experiments. This reaction appears to be pressure-independent. It should be mentioned that at the G2M (CC1) level, the heat of formation for HO_2 was predicted to be 4.2 kcal/mol, which is in close agreement with the value of 4.32 kcal/mol (Ref. 55) based on the CBS//CCSD(T)/aug-cc-pVDZ calculation and also with the most recent experimental value, 4.0 ±0.8 kcal/mol (Ref. 83) and 3.9±0.5 kcal/mol.[84]

2. Rate constants for the reaction $HO+NO_2 \rightarrow HONO_2$ (HOONO) and product branching ratios

a. Pressure dependence: The $HO+NO_2$ reaction has been studied by numerous research groups[20–50,79,85–87] in the past. Experimentally, Hippler, Troe, and co-workers[23,27,30] extensively studied the pressure dependence in the recombination reaction of HO and NO_2 with different third-bodies. In this work, we mainly compare our predicted values with experimentally measured data.

Figures 6(a) and 6(b) compare the pressure dependence of our predicted values and experimental data at 300 and 400 K with He as a third-body. The predicted rate constants and branching ratios for the formation of HOONO and $HONO_2$ under different pressures at 300 and 400 K are also summarized in Table II. The results show that below 1 atm, formation of HOONO is <2.4% and 2.0% at 300 and 400 K, respectively, which is consistent with Troe's predicted result that "formation of HOONO amounts to less than about 2.5% of the reaction between 200 and 400 K at pressure up to 1 bar."[85] The results obtained by Golden and Smith[86] using hindered-Gorin RRKM calculations indicate that *k*

TABLE II. Rate constants and branching ratios for the formation of $HONO_2$ and HOONO at different pressure at 300 and 400 K in units of $cm^3\ molecule^{-1}\ s^{-1}$.

Pressure (Torr)	k_{HONO2}	k_{HOONO}	k_{total}	k_{HOONO}/k_{total}
		300 K		
1.00E−04	5.87E−18	4.38E−20	5.91E−18	7.41E−03
5.00E+00	2.24E−13	2.16E−15	2.26E−13	9.55E−03
20	7.23E−13	8.30E−15	7.31E−13	1.13E−02
5.00E+01	1.50E−12	1.96E−14	1.52E−12	1.29E−02
1.00E+02	2.51E−12	3.71E−14	2.55E−12	1.46E−02
3.00E+02	5.31E−12	1.00E−13	5.41E−12	1.85E−02
5.00E+02	7.29E−12	1.59E−13	7.45E−12	2.13E−02
7.60E+02	9.28E−12	2.31E−13	9.51E−12	2.43E−02
7.60E+03	2.57E−11	1.60E−12	2.73E−11	5.86E−02
3.80E+04	3.76E−11	5.24E−12	4.28E−11	1.22E−01
7.60E+05	4.64E−11	2.70E−11	7.34E−11	3.68E−01
7.60E+06	4.72E−11	4.98E−11	9.70E−11	5.13E−01
7.60E+07	4.73E−11	5.93E−11	1.07E−10	5.56E−01
		400 K		
1.00E−04	2.21E−18	1.63E−20	2.23E−18	7.32E−03
5.00E+00	8.93E−14	8.05E−16	9.01E−14	8.93E−03
20	3.01E−13	3.12E−15	3.04E−13	1.03E−02
5.00E+01	6.44E−13	7.50E−15	6.52E−13	1.15E−02
1.00E+02	1.11E−12	1.44E−14	1.12E−12	1.28E−02
3.00E+02	2.50E−12	4.00E−14	2.54E−12	1.57E−02
5.00E+02	3.54E−12	6.43E−14	3.60E−12	1.78E−02
7.60E+02	4.64E−12	9.44E−14	4.73E−12	1.99E−02
7.60E+03	1.53E−11	7.12E−13	1.60E−11	4.45E−02
3.80E+04	2.54E−11	2.54E−12	2.79E−11	9.09E−02
7.60E+05	3.56E−11	1.65E−11	5.21E−11	3.17E−01
7.60E+06	3.67E−11	3.73E−11	7.40E−11	5.04E−01
7.60E+07	3.69E−11	4.97E−11	8.66E−11	5.74E−01

(HOONO)/k ($HONO_2$) may be as high as 15% under the atmospheric condition. Very recent experimental results of Nizkodorov *et al.*[24] show that the formation of HOONO is around 5±3% at 253 K in 20 Torr of a N_2/He mixture, which is close to our predicted value. From Figs. 6(a) and 6(b), and Table II we see that at higher pressures, formation of HOONO becomes competitive and noticeable, only the sum of k (HOONO) and k ($HONO_2$) can well reproduce the experimental results of Hippler and co-workers.[23] At pressures over 7.6×10^6 Torr, formation of HOONO becomes dominant at both 300 and 400 K. In the work of Golden and Smith,[86] k (HOONO) already becomes dominant at 300 K when the pressure (in N_2) reaches 7.6×10^3 Torr (see Table II of Ref. 86). It should be mentioned that the effect of pressure appears to be slightly $\langle\Delta E_{down}\rangle$-dependent. Experimentally, the energy transfer parameters ($\langle\Delta E_{down}\rangle$) are not often available, one way to estimate the parameters is to fit the experimental fall-off curves obatined at different temperatures. In the above calculation, $\langle\Delta E_{down}\rangle=100$ and 140 cm^{-1} were employed for 300 and 400 K, respectively, which can well reproduce the experimental results. The low-pressure (in He) and high-pressure rate constants for the formation of $HONO_2$ and HOONO in the temperature of 200–2000 K can be, respectively, expressed as

$$k^0\ (HONO_2)=3.32\times10^{-6}\ T^{-8.8}\times\exp(-1569/T)\ cm^6\ molecule^{-2}\ s^{-1},$$

$$k^0\ (HOONO)=3.15\times10^{2}\ T^{-12.3}\times\exp(-2585/T)\ cm^6\ molecule^{-2}\ s^{-1},$$

$$k^\infty\ (HONO_2)=4.74\times10^{-9}\ T^{-0.82}\times\exp(21/T)cm^3\ molecule^{-1}\ s^{-1},$$

$$k^\infty(HOONO)=1.71\times10^{-10}\ T^{-0.24}\times\exp(100/T)cm^3\ molecule^{-1}\ s^{-1}.$$

b. Temperature dependence: Figure 7 displays the predicted and experimental third-order rate constants for the reaction $HO+NO_2+M\rightarrow HONO_2+M$ with N_2 as a third-body. The figure shows that our predicted values reasonably agree with existing experimental data (as cited in the caption). The third-order rate constant can be presented as

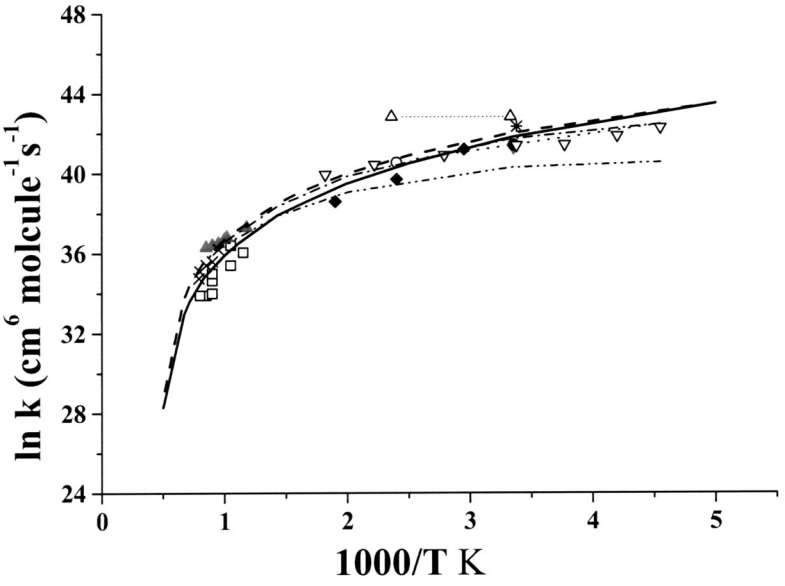

FIG. 7. Comparison of predicted third-order rate constants for $HO+NO_2$ with experimental values and some previously predicted data. Thick solid and dashed lines are predicted values with N_2 and Ar as third-bodies, respectively. Dashed–dotted and dashed–dotted–dotted lines are taken from the equations of Refs. 87 and 31, respectively. □, Ref. 21; -▲-, Ref. 46; ♦, Ref. 42; ▼, Ref. 35; ○, Ref. 29; ●, Ref. 33; ×, Ref. 22; ▽, Ref. 42; *, Ref. 42; △, Ref. 49.

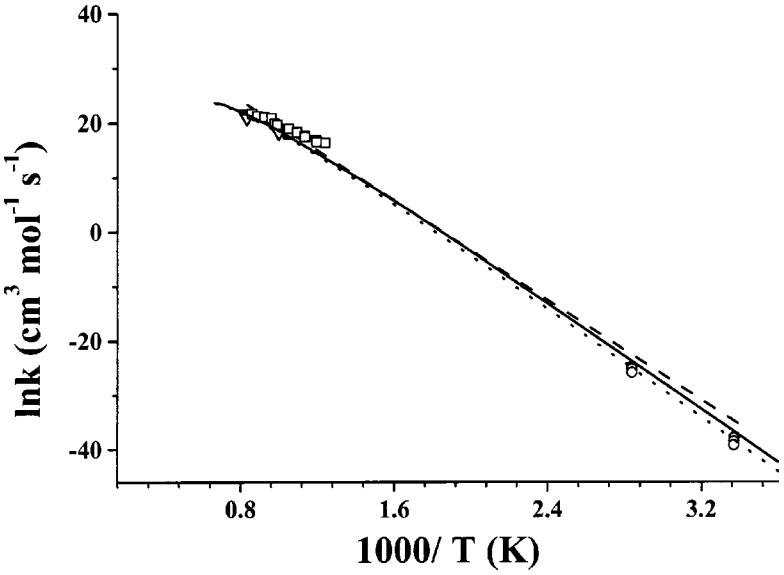

FIG. 8. Comparison of the predicted second-order decomposition rate constant of HNO_3 with experimental values in Ar. Solid and dotted lines are the predicted values at 10^{-4} and 500 Torr, respectively; dashed line is taken from the equation in Ref. 46 (for the low-pressure limit between 295 and 1200 K). ▽, Ref. 88 (2–5 Torr); □, Ref. 89 (500 Torr); ○, Ref. 36 (14–700 Torr).

$$k^0\ (\mathrm{HONO_2}) = 2.95\times 10^{-5}\ T^{-8.97} \times \exp(-1708/T)\ \mathrm{cm^6\ molecule^{-1}\ s^{-1}}.$$

3. Rate constants for the decomposition of HNO_3

The calculated second-order rate constants for the decomposition of HNO_3 are plotted as a solid line in Fig. 8 for comparison with available literature data. For this barrierless dissociation process, the Morse potential with $\beta = 2.60\ \text{Å}^{-1}$ was used to represent the potential energy along the minimum energy path.[58] It is evident from the figure that our predicted values (solid line) agree well with the experimental results of Glänzer and Troe[46] in the temperature range of 295–1200 K given by the dashed line; the values at 247–352 K (open circles)[36] are obtained by converting the reaction rates of $OH + NO_2 \rightarrow HNO_3$ (at 14–700 Torr in Ar) using our predicted equilibrium constant, $K_{eq} = 4.10\times 10^{-31}\ T^{1.07} \exp(26026.7/T)\ \mathrm{cm^3\ molecule^{-1}}$. Calculated values at 500 Torr (dotted line) agree well with those experimental data. Predicted values also agree closely with the available high temperature shock tube data (see the citation in the caption).

The high- and low-pressure (in Ar) limit decomposition rates based on the G2M energies can be expressed, respectively, by

$$k_d^{\infty}\ (\mathrm{HNO_3}) = 2.30\times 10^{23}\ T^{-2.27} \exp(-26320/T)\ \mathrm{s^{-1}},$$

$$k_d^{0}\ (\mathrm{HNO_3}) = 1.27\times 10^{15}\ T^{-6.55} \exp(-26040/T)\ \mathrm{cm^3\ molecule^{-1}\ s^{-1}}.$$

IV. CONCLUSIONS

The PES for the $HO_2 + NO$ reaction has been elucidated at the G2M(CC1)//6-311+G($3df$,$2p$) level of theory. The rate constants for the forward and reverse processes have been calculated under different conditions. The results show that the formation of $HO + NO_2$ from $HO_2 + NO$ is pressure-independent below 10 atm; the decomposition of HOONO to $HO + NO_2$ is more favorable than its isomerization to $HONO_2$ due to the high barrier for the latter process. The reverse reaction $HO + NO_2 \rightarrow HONO_2$ (HOONO) appears to be strongly pressure-dependent; below 1 atm, the yield of HOONO was predicted to be $<2.5\%$; however, at higher pressures, the formation of HOONO becomes competitive and only the sum of the rate constants for the two channels can well reproduce the experimental data. All of the predicted results, including those for the unimolecular decomposition of HNO_3, agree closely with experimental values.

ACKNOWLEDGMENTS

This work is sponsored by the Office of Naval Research under Contract No. N00014–02-1-0133, Dr. J. Goldwasser program manager. Acknowledgment is also made to the Cherry L. Emerson Center of Emory University for the use of its resources, which are in part supported by a National Science Foundation Grant No. CHE-0079627 and an IBM Shared University Research Award.

[1] B. Bohn and C. Zetzsch, J. Chem. Soc., Faraday Trans. **94**, 1203 (1998).
[2] W. B. DeMore, S. P. Sander, D. M. Golden, R. F. Hampson, M. J. Kurylo, C. J. Howard, A. R. Ravishankara, C. E. Kolb, and M. J. Molina, JPL Publication 97-4 (1997).
[3] R. Atkinson, D. L. Baulch, R. A. Cox, R. F. Hampson, Jr., J. A. Kerr, M. J. Rossi, and J. Troe, J. Phys. Chem. Ref. Data **26**, 1329 (1997).
[4] J. V. Seeley, R. F. Meads, M. J. Elrod, and M. J. Molina, J. Phys. Chem. **100**, 4026 (1996).
[5] P. D. Lightfoot, R. A. Cox, J. N. Crowley, M. Destriau, G. D. Hayman, M. E. Jenkin, G. K. Moortgat, and F. Zabel, Atmos. Environ., Part A **26**, 1805 (1992).
[6] A. A. Jemi-Alade and B. A. Thrush, J. Chem. Soc., Faraday Trans. **86**, 3355 (1990).
[7] V. B. Rozenshtein, Y. M. Gershenzon, S. D. Il'in, and O. P. Kishkovitch, Chem. Phys. Lett. **112**, 473 (1984).
[8] J. J. Margitan, J. Phys. Chem. **88**, 3314 (1984).
[9] B. A. Thrush and J. P. T. Wilkinson, Chem. Phys. Lett. **81**, 1 (1981).
[10] C. J. Howard, J. Am. Chem. Soc. **102**, 6937 (1980).
[11] W. Hack, A. W. Preuss, F. Temps, H. Gg. Wagner, and K. Hoyermann, Int. J. Chem. Kinet. **12**, 851 (1980).
[12] I. Glaschick-Schimpf, A. Leiss, P. B. Monkhouse, U. Schurath, K. H. Becker, and E. H. Fink, Comm. Eur. Communities Rpt. 6621 **1**, 122 (1980).

[13] J. P. Burrows, D. I. Cliff, G. W. Harris, B. A. Thrush, and J. P. T. Wilkinson, Proc. R. Soc. London, Ser. A **368**, 463 (1980).
[14] M. T. Leu, J. Chem. Phys. **70**, 1662 (1979).
[15] C. J. Howard, J. Chem. Phys. **71**, 2352 (1979).
[16] R. Simonaitis and J. Heicklen, Int. J. Chem. Kinet. **10**, 67 (1978).
[17] C. J. Howard and K. M. Evenson, Geophys. Res. Lett. **4**, 437 (1977).
[18] R. A. Cox and R. G. Derwent, J. Photochem. **4**, 139 (1975).
[19] W. A. Payne, L. J. Stief, and D. D. Davis, J. Am. Chem. Soc. **95**, 7614 (1973).
[20] R. K. Hanson and S. Salimian, *Combustion Chemistry*, edited by W. C. Gardiner, Jr. (Springer-Verlag, New York, 1984).
[21] V. Y. Basevich and S. M. Kogarko, Bull. Acad. Sci. USSR, Phys. Ser. (Engl. Transl.) **27**, 1988 (1979).
[22] M. S. Woolridge, R. K. Hanson, and C. T. Bowman, in *Shockwaves at Marseille II*, edited by R. Brun and L. Z. Dumitrescu (Springer-Verlag, Berlin, 1995), p. 83.
[23] (a) H. Hippler, S. Nasterlack, and F. Striebel, Phys. Chem. Chem. Phys. **4**, 2959 (2002); (b) H. Hippler, S. Nasterlack, F. Striebel, and D. M. Golden, in *Proceeding of the 5th International Conference on Chemical Kinetics* (NIST, Gaithersburg, Maryland, 2001).
[24] S. A. Nizkorodov and P. O. Wennberg, J. Phys. Chem. A **106**, 855 (2002).
[25] N. M. Donahue, R. Mohrschladt, T. J. Dransfield, J. G. Anderson, and M. K. Dubey, J. Phys. Chem. A **105**, 1515 (2001).
[26] T. J. Dransfield, N. M. Donahue, and J. G. Anderson, J. Phys. Chem. A **105**, 1507 (2001).
[27] D. Fulle, H. F. Hamann, H. Hippler, and J. Troe, J. Chem. Phys. **108**, 5391 (1998).
[28] N. M. Donahue, M. K. Dubey, R. Mohrschladt, K. L. Demerjian, and J. G. Anderson, J. Geophys Res. **102**, 6159 (1997).
[29] R. Atkinson, D. L. Baulch, R. A. Cox, R. F. Hampson, Jr., J. A. Kerr, M. J. Rossi, and J. Troe, J. Phys. Chem. Ref. Data **26**, 1329 (1997).
[30] R. Forster, M. Frost, D. Fulle, H. F. Hamann, H. Hippler, A. Schlepegrell, and J. Troe, J. Chem. Phys. **103**, 2949 (1995).
[31] W. Tsang and J. T. Herron, J. Phys. Chem. Ref. Data **20**, 609 (1991).
[32] J. B. Burkholder, P. D. Hammer, and C. J. Howard, J. Phys. Chem. **91**, 2136 (1987).
[33] J. P. Burrows, T. J. Wallington, and R. P. Wayne, J. Chem. Soc., Faraday Trans. 2 **79**, 111 (1983).
[34] J. S. Robertshaw and I. W. M. Smith, J. Phys. Chem. **86**, 785 (1982).
[35] L. G. Anderson, J. Phys. Chem. **84**, 2152 (1980).
[36] P. H. Wine, N. M. Kreutter, and A. R. Ravishankara, J. Phys. Chem. **83**, 3191 (1979).
[37] I. M. Campbell and P. E. Parkinson, J. Chem. Soc., Faraday Trans. 1 **75**, 2048 (1979).
[38] R. Zellner, Ber. Bunsenges. Phys. Chem. **82**, 1172 (1978).
[39] C. Anastasi and I. W. M. Smith, J. Chem. Soc., Faraday Trans. 1 **74**, 1693 (1978).
[40] K. Erler, D. Field, R. Zellner, and I. W. M. Smith, Ber. Bunsenges. Phys. Chem. **81**, 22 (1977).
[41] R. Atkinson, R. A. Perry, J. N. Pitts, Jr., J. Chem. Phys. **65**, 306 (1976).
[42] C. Anastasi and I. W. M. Smith, J. Chem. Soc., Faraday Trans. 1 **72**, 1459 (1976).
[43] C. Anastasi, P. P. Bemand, and I. W. M. Smith, Chem. Phys. Lett. **37**, 370 (1976).
[44] G. W. Harris and R. P. Wayne, J. Chem. Soc., Faraday Trans. 1 **71**, 610 (1975).
[45] C. J. Howard and K. M. Evenson, J. Chem. Phys. **61**, 1943 (1974).
[46] K. Glänzer and J. Troe, Ber. Bunsenges. Phys. Chem. **78**, 71 (1974).
[47] J. G. Anderson, J. J. Margitan, and F. Kaufman, J. Chem. Phys. **60**, 3310 (1974).
[48] A. A. Westenberg and N. DeHaas, J. Chem. Phys. **57**, 5375 (1972).
[49] R. Simonaitis and J. Heicklen, Int. J. Chem. Kinet. **4**, 529 (1972).
[50] J. G. Anderson and F. Kaufman, Chem. Phys. Lett. **16**, 375 (1972).
[51] M. P. McGrath, M. M. Francl, M. S. Rowland, and W. J. Hehre, J. Phys. Chem. **92**, 5352 (1988).
[52] Y. M. Li and J. S. Francisco, J. Chem. Phys. **113**, 7976 (2000).
[53] W. H. Koppenol and L. Klasinc, Int. J. Quantum Chem., Quantum Chem. Symp. **20**, 1 (1993).
[54] H. H. Tsai, T. P. Hamilton, J. H. M. Tsai, M. V. D. Woerd, J. G. Harrison, M. J. Jablonsky, J. S. Beckman, and W. H. Koppenol, J. Phys. Chem. **100**, 15087 (1996).
[55] D. A. Dixon, D. Feller, C. G. Zhan, and J. S. Francisco, J. Phys. Chem. A **106**, 3191 (2002).
[56] M. P. McGrath and F. S. Rowland, J. Phys. Chem. **98**, 106 (1994).
[57] R. Sumathi and S. D. Peyerimhoff, J. Chem. Phys. **107**, 1872 (1997).
[58] D. Chakraborty, J. Park, and M. C. Lin, Chem. Phys. **231**, 39 (1998).
[59] H. W. Jin, Z. Z. Wang, Q. S. Li, X. R. Huang, J. Mol. Struct.: THEOCHEM **624**, 115 (2003).
[60] A. M. Mebel, K. Morokuma, and M. C. Lin, J. Chem. Phys. **103**, 7414 (1995).
[61] A. D. Becke, J. Chem. Phys. **98**, 5648 (1993).
[62] A. D. Becke, J. Chem. Phys. **96**, 2155 (1992).
[63] A. D. Becke, J. Chem. Phys. **97**, 9173 (1992).
[64] C. Lee, W. Yang, and R. G. Parr, Phys. Rev. B **37**, 785 (1988).
[65] C. Gonzalez and H. B. Schlegel, J. Phys. Chem. **90**, 2154 (1989).
[66] M. J. Frisch, G. W. Trucks, H. B. Schlegel *et al.*, GAUSSIAN 98, Revision A.1, Gaussian, Inc., Pittsburgh, PA, 1998.
[67] S. J. Klippenstein, A. F. Wagner, R. C. Dunbar, D. M. Wardlaw, and S. H. Robertson, VARIFLEX, Version 1.00, 1999.
[68] R. G. Gilbert and S. C. Smith, *Theory of Unimolecular and Recombination Reactions* (Blackwell Scientific, Carlton, Australia, 1990).
[69] K. A. Holbrook, M. J. Pilling, and S. H. Robertson, *Unimolecular Reactions* (Wiley, New York, 1996).
[70] V. Mokrushin, V. Bedanov, W. Tsang, M. R. Zachariah, and V. D. Knyazev, CHEMRATE, Version 1.19, National Institute of Standards and Technology, Gaithersburg, Maryland, 2002.
[71] W. J. Lo and Y. P. Lee, J. Chem. Phys. **101**, 5494 (1994).
[72] R. S. Zhu, Z. F. Xu, and M. C. Lin, J. Chem. Phys. **116**, 7452 (2002).
[73] R. S. Zhu and M. C. Lin, J. Chem. Phys. **118**, 4094 (2003).
[74] R. S. Zhu and M. C. Lin, J. Phys. Chem. A **106**, 8386 (2002).
[75] Z.-F. Xu, R. Zhu, and M. C. Lin, J. Phys. Chem. A **107**, 1040 (2003).
[76] R. S. Zhu and M. C. Lin, J. Chem. Phys. **118**, 8645 (2003).
[77] R. S. Zhu and M. C. Lin, J. Chem. Phys. **118**, 4094 (2003).
[78] M. T. Nguyen, H. T. Le, B. Hajgató, T. Veszprémi, and M. C. Lin, J. Phys. Chem. A **107**, 4286 (2003).
[79] D. M. Matheu and W. H. Green, Jr., Int. J. Chem. Kinet. **32**, 245 (2000).
[80] H. Hippler, J. Troe, and H. J. Wendelken, J. Chem. Phys. **78**, 6709 (1983).
[81] C.-C. Hsu, A. M. Mebel, and M. C. Lin, J. Chem. Phys. **105**, 2346 (1996).
[82] D. Chakraborty, C.-C. Hsu, and M. C. Lin, J. Chem. Phys. **109**, 8887 (1998).
[83] M. Litorja and B. Ruscic, J. Electron Spectrosc. Relat. Phenom. **97**, 131 (1998).
[84] T. M. Ramond, S. J. Blanksby, S. Kato, V. M. Bierbaum, G. E. Davico, R. L. Schwartz, W. C. Lineberger, and G. B. Ellison, J. Phys. Chem. A **106**, 9641 (2002).
[85] J. Troe, Int. J. Chem. Kinet. **33**, 878 (2001).
[86] D. M. Golden and G. P. Smith, J. Phys. Chem. A **104**, 3991 (2000).
[87] G. P. Smith and D. M. Golden, Int. J. Chem. Kinet. **10**, 489 (1978).
[88] Yu M. Gershenzon, A. P. Dement'ev, and A. B. Nalbandyan, Kinet. Katal. **20**, 565 (1979).
[89] H. Harrison, H. S. Johnston, and E. R. Hardwick, J. Am. Chem. Soc. **84**, 2478 (1962).